

# Structural analysis of a Ti–Al–silicate catalyst for propylene oligomerization

L. FORNI\*, M. PELOZZI

*Dipartimento di Chimica Fisica ed Elettrochimica Università di Milano, Via C. Golgi 19, 20133 Milano, Italy*

A. CARATI, A. GIUSTI, R. MILLINI

*Eniricerche SpA, Via Maritano 26, 20097 S. Donato Milanese, Italy*

The present Ti–Al–silicalite catalyst showed the typical MFI structure, in which titanium is included in the silicalite crystalline framework. Microcrystals (0.03 to 0.05  $\mu\text{m}$ ) of the zeolite are stuck together to form pseudo-spherical, berry-like, strong conglomerates, approximately 0.1 to 0.5  $\mu\text{m}$  in size. The catalyst proved to be more active than a similar ZSM5 sample for propylene oligomerization, which practically stops at dimers and trimers. However, the latter undergo further cleavage to  $\text{C}_4$  and  $\text{C}_5$ , which in turn react with  $\text{C}_3$  to give  $\text{C}_7$  and  $\text{C}_8$  products.

## 1. Introduction

Oligomerization and/or co-oligomerization of light ( $\text{C}_2$ – $\text{C}_5$ ) olefins is a well-known upgrading catalytic process, by means of which a wide variety of intermediates are produced, largely employed for the preparation of special resins, detergents, plastifiers, etc. Interest in the subject has stimulated a continuous production of research reports and of some excellent review papers, especially over the last two decades [1–9]. The possibility of directing the oligomerization of a given olefin towards a particular product relies completely on the nature and structure of the catalyst. In the case of propylene, for instance, supported alkali metals lead to 4-methyl-1-pentene with over 95% selectively [10–14], while acidic catalysts, such as phosphoric acid supported on kieselguhr or Ni–zeolite catalysts [15, 16], lead to a complex mixture of trimers, tetramers and higher, largely employed for the preparation of nonyl- or dodecyl-benzenes. Among the propylene and butenes, oligomers or co-oligomers which are particularly interesting are the linear  $\text{C}_8$ – $\text{C}_{12}$  olefins, which can be obtained in good yields by exploiting the unique shape-selectivity characteristic of zeolites, especially of the pentasil class.

A study of the catalytic properties of some Ti–Al–silicalite-type zeolites prepared in these laboratories produced evidence of their good activity in the oligomerization of propylene [17], thus prompting a deeper investigation of such solids, to obtain more information on their structure and properties. The present paper reports the results of the structural analysis of a typical representative sample of such catalysts.

## 2. Experimental procedure

The Ti–Al–silicalite sample (ER1) was prepared as

described [18] from mixtures containing tetraethyl-orthosilicate (Dynasil A), aqueous tetrapropylammonium hydroxide (TPAOH), tetraethylorthotitanate (Merck 98%), aluminium isopropoxide (Fluka 99.9999%) and water at the following molar ratios:  $\text{SiO}_2/\text{Al}_2\text{O}_3 = 300$ ,  $\text{SiO}_2/\text{TiO}_2 = 20$ ,  $\text{TPAOH}/\text{SiO}_2 = 0.25$ ,  $\text{H}_2\text{O}/\text{SiO}_2 = 40$ . The hydrothermal crystallization was carried out at 100 °C and autogenous pressure for 5 d. The solid obtained was filtered, washed, dried and calcined in air at 500 °C for 5 h. For comparison, an Al–ZSM5 sample (ER2) was also prepared according to a Mobil patent [19]. The protonated forms were obtained by repeated exchange with 5 wt % aqueous ammonium acetate at 80 °C, followed by drying and calcination for 5 h in air at 550 °C.

The chemical composition was obtained by the inductive coupling plasma technique (for titanium and aluminium), or by gravimetry (for silicon). The molar ratios of the main components in the two samples are shown in Table I. The crystalline nature of the solids was analysed by X-ray diffraction (XRD),  $\text{CuK}\alpha$  radiation ( $\lambda = 0.154178$  nm) on a computer-controlled Philips diffractometer, equipped with a pulse-height analyser. The morphology of the zeolite was determined by TEM, by means of a Philips TEM 450 instrument. The specimens were prepared by embedding the samples in resin, followed by ultrathin slicing (30 to 70 nm). Pore size and pore volume distribution

TABLE I Molar ratios of the main components in the catalysts

Catalyst	ER1	ER2
$\text{SiO}_2/\text{Al}_2\text{O}_3$	160	26
$\text{SiO}_2/\text{TiO}_2$	131	–

\* Author to whom all correspondence should be addressed.

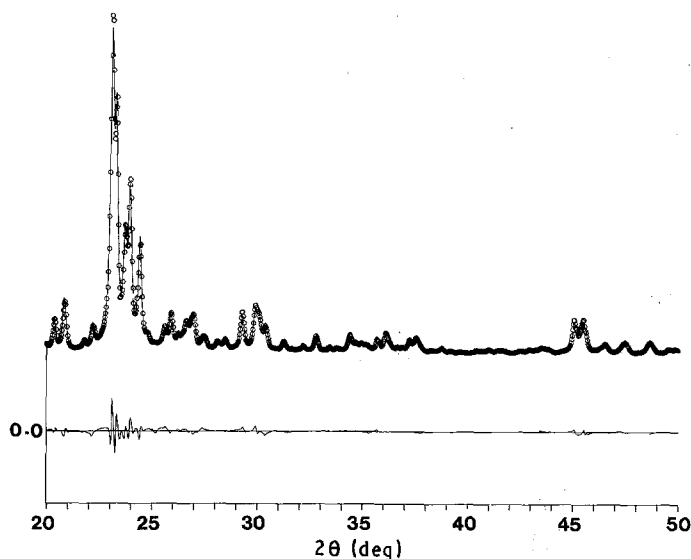


Figure 1 Experimental (○), calculated (—) and difference pattern (lower line) obtained during the Rietveld refinement of the ER1 sample structure.

in the meso-macro pore range (3.7 to 7500 nm pore radius) were determined by mercury intrusion using a model 2000 C. Erba porosimeter. Infrared spectra were recorded at room temperature by means of a Perkin Elmer 1730 Fourier transform spectrophotometer. The wafers were prepared at 0.8 wt % dilution in KBr.

The catalytic oligomerization of propylene was carried out in a fixed-bed continuous microreactor assembly, previously described [17]. Samples of fresh catalyst (100 to 500 g, particle size 0.42 to 0.85 mm) were charged, diluted in quartz chips to avoid hot spots. A mixture of propylene, diluted (30 vol %) in nitrogen was fed, and temperature was controlled by means of a coaxial thermocouple, connected to a PID TRC. All the experiments were carried out at atmospheric total pressure. On-line gas chromatographic analysis of the reaction products was performed by means of an FID HP 5880 gas chromatograph equipped with a 4.5 m long Porapak QS column. Helium ( $30 \text{ cm}^3 \text{ min}^{-1}$ ) was used as carrier gas.

### 3. Results and discussion

#### 3.1. X-ray diffraction

Inspection of the XRD powder patterns of the ER1 sample indicated the typical pentasil-type framework structure. The pattern of ER2 was quite different, being characterized by broad reflections, a higher degree of line convolution and different relative intensities. These features can originate from both reduced crystal size and, more likely, the presence of a defective structure. The ER1 sample was characterized by an orthorhombic lattice symmetry, consistent with the presence of titanium and aluminium in the framework.

Further experimental evidence, confirming the actual incorporation of titanium and aluminium in the silicalite framework derives from the accurate determination of the unit-cell volume. It is known [20] that unit-cell size can be employed as a means for the determination of the framework composition in various pentasil-type zeolites, such as B-, Ti- and

Al-silicalites (ZSM5) and that a linear correlation may be obtained between the unit-cell volume and the boron, titanium and aluminium content. In particular, an expansion of the unit-cell volume was observed in the case of titanium-silicalite [20] and H-ZSM5 [21], due to the substitution of silicon ions with bulkier ions, while the opposite trend was observed for boron-silicalite [22], because of the smaller size of the boron ion, with respect to silicon. However, the usual procedure for the evaluation of unit-cell volume, consisting of the least-squares fit to the interplanar spacing of some selected single strong reflections was not easily applicable in the case of ER1, because of the high degree of line convolution in the X-ray powder pattern. Therefore a new approach was employed based on the Rietveld method [23], which allows refinement of the structural parameters, including atomic positions, by taking into account the full profile of the diffraction pattern. The refinements were carried out using the PREFIN program [24]. Peak shapes were described through the Pearson VII profile function. The atomic parameters reported for the crystal structure of ZSM5 [25] were used. These parameters were kept fixed while refining the unit-cell parameters, the peak function parameters, the background intensity values and the zero correction. Intensity disagreement factors ( $R_{wp}$ ) obtained were 5.6% (ER1) and 6.2% (ER2). Fig. 1 shows the application of this procedure to the refinement of the ER1 sample structure.

The expected expansion of the unit-cell volume was effectively observed. Silicalite, the pure silica parent structure, is characterized by a unit-cell volume of  $5.3418 \text{ nm}^3$  [20], while volumes  $5.3685$  and  $5.3718 \text{ nm}^3$  were calculated for ER1 and ER2 samples, respectively.

#### 3.2. TEM analysis and mercury penetration porosimetry

Transmission electron micrographs revealed a particular structure (Figs 2 and 3), consisting of pseudo-spherical, berry-like conglomerates (0.1 to 0.4  $\mu\text{m}$  diameter) of by at least one order of magnitude smaller (0.01 to 0.03  $\mu\text{m}$ ) zeolitic microcrystals.

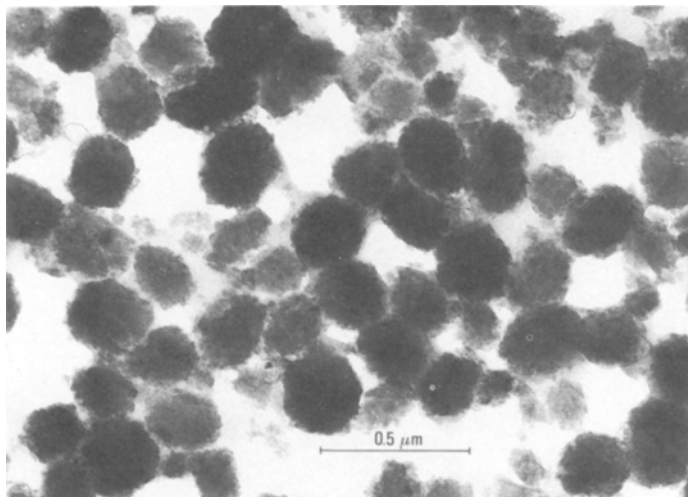


Figure 2 Typical transmission electron micrograph of the ER1 sample, showing the berry-like structure of zeolitic crystals conglomerates.

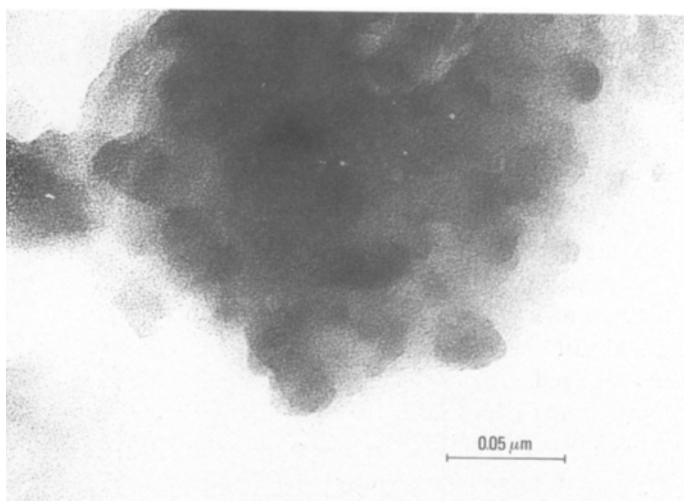


Figure 3 Enlargement of a single "berry" of Fig. 2, showing the berry-seed-like morphology of the zeolitic crystals.

The information collected by the mercury penetration porosimetry (Fig. 4 and Table II) after pressing the sample at two different pelleting pressures (2 and 5 t cm<sup>-2</sup>, respectively) followed by crushing and sieving to 50 to 80 mesh, showed that the decrease in the pore volume brought about by pelleting is due essentially to a decrease in macroporosity, the mesopore volume remaining unchanged. Thus the berry-like particles are quite compact, with very small free volume between their "seeds".

### 3.3. Mid-infrared spectral analysis

The mid-infrared spectrum of the ER1 sample (Fig. 5) shows the characteristic features of the MFI structure, with absorption bands at ~ 1230, 1100, 800, 500 and 450 cm<sup>-1</sup> [26], together with a new band at

970 cm<sup>-1</sup>. This latter band is related to the presence of structural titanium [20]. The assignment is based on comparison with Raman spectra observed for TiO<sub>2</sub>-SiO<sub>2</sub> glasses with less than 20% TiO<sub>2</sub>. In these materials a strong band at ~ 950 cm<sup>-1</sup> is present, associated with vibrational mode involving SiO<sub>4</sub> units linked to TiO<sub>4</sub> in a polymeric structure [27].

### 3.4. Catalytic behaviour

The results of catalytic activity tests have been expressed in terms of conversion *C* (mol % propylene fed) and selectivity *S<sub>i</sub>* (mol % reacted propylene, transformed into the *i*th product). The data (Table III) show the ER1 catalyst is more active than ER2. In

TABLE II Pore volume data from mercury intrusion analysis

Pelleting press (t cm <sup>-2</sup> )	Pore volume (cm <sup>3</sup> g <sup>-1</sup> )	
	Mesopores 3.7 ≤ <i>r<sub>p</sub></i> ≤ 30 nm	Macropores 30 nm ≤ <i>r<sub>p</sub></i> ≤ 7500 nm
2	0.23	0.41
5	0.23	0.39

TABLE III Conversion of propylene. *T* = 550 K, propylene WHSV = 24 h<sup>-1</sup> and feeding partial pressure 0.14 × 10<sup>5</sup> Pa

Time on stream (h)	Conversion of propylene (mol %)	
	ER1	ER2
0	84.0	64.8
10	77.3	62.5
20	75.5	61.1
30	73.1	58.8
40	71.7	54.7

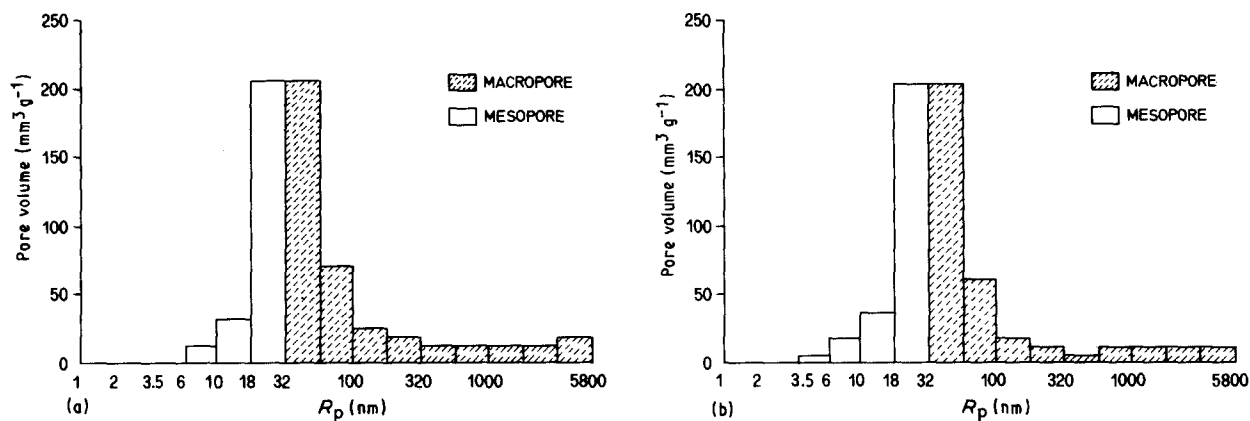


Figure 4 Pore size distribution from mercury intrusion analysis. Pelleting pressure: (a) and (b)  $5 \text{ t cm}^{-2}$ .

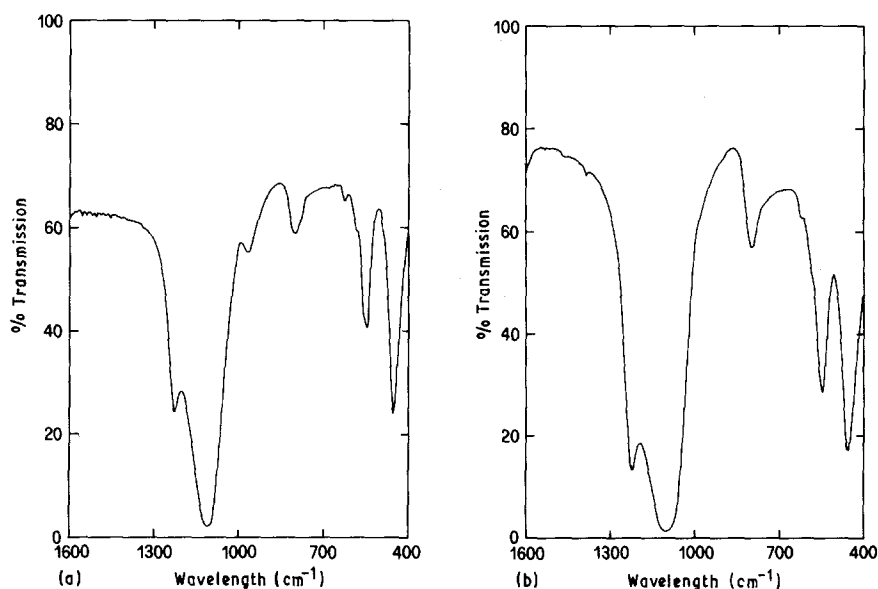


Figure 5 Infrared spectrum of (a) ER1 and (b) ER2 sample.

addition, the relative abundance of the products (Table IV) shows that the oligomerization promoted by ER1 is very likely essentially a dimerization and trimerization. However, the  $C_9$  trimers, diffusing much less rapidly than  $C_6$ , undergo a practically complete cleavage to  $C_4 + C_5$  and the latter, in turn, react with  $C_3$  to give  $C_7$  and  $C_8$  products, respectively.

This behaviour in oligomerization may be considered typically due to the framework structure of these pentasil-type zeolites, the pore size of which determines a strong shape-selectivity effect, preventing the formation of bulkier molecules, such as tetramers or pentamers, and transforming the trimers to lighter molecules before they can find their way out of the pore system of the catalyst.

#### 4. Conclusions

The Ti-Al-silicate sample examined showed the typical MFI structure, in which titanium is included in the crystalline framework. The microcrystals of the zeolitic solid are stuck together to form small berry-like conglomerates approximately one order of magnitude larger than their crystalline seeds. These berry-like conglomerates are quite compact, with a very small free volume between the seeds. In its decationated (protonated) form the catalyst is more active than a similar ZSM5-based one towards propylene oligomerization. The latter is essentially a dimerization-trimerization reaction, followed by cleavage of trimers to  $C_4 + C_5$ , which further react with propylene to give  $C_7$  and  $C_8$  products.

TABLE IV Selectivity of ER1 catalyst to oligomerization products. Reaction conditions as for Table III

Time on stream (h)	$C_1$ (%)	$C_2$ (%)	$C_3$ (%)	$C_4$ (%)	$C_5$ (%)	$C_6$ (%)	$C_7$ (%)	$C_8$ (%)	$C_9$ (%)
0	0	0.05	0.5	30.7	29.9	18.8	12.5	7.5	tr
40	0	0.03	0.4	30.6	28.4	18.4	13.0	8.0	1.2

## Acknowledgements

The authors thank Mr M. Buroni and Dr. F. Bazzano for TEM and elemental analysis, respectively.

## References

1. J. HABELSHAW, In "Propylene and its Industrial Derivatives", edited by E. G. Hancock (Benn, London, 1973) p. 115.
2. M. SITTIG, "Handbook of Catalyst Manufacture" (Noyes Data, Park Ridge, 1978) p. 358.
3. I. E. MAXWELL, *Adv. Catal.* **31** (1982) 1.
4. J. P. VAN DEN BERG, J. P. WOLTHUIZEN, A. D. H. CLAGUE, G. R. HAYS, R. HUIS and J. H. C. VAN HOOFF, *J. Catal.* **80** (1983) 130.
5. J. C. Q. FLETCHER, M. KOJIMA and C. T. O'CONNOR, *Appl. Catal.* **28** (1986) 181.
6. R. L. ESPINOZA, C. P. NICOLAIDES, C. J. KORF and R. SNEL, *ibid.* **31** (1987) 259.
7. C. T. O'CONNOR, L. L. JACOBS and M. KOJIMA, *ibid.* **40** (1988) 277.
8. R. J. QUANN, L. A. GREEN, S. A. TABAK and F. J. KRAMBECK, *Ind. Engng Chem. Res.* **27** (1988) 565.
9. J. HEVELING, A. VAN DER BEEK and M. PENDER, *Appl. Catal.* **42** (1988) 325.
10. L. FORNI and R. INVERNIZZI, *Ind. Engng Chem. Process Des. Dev.* **12** (1973) 455.
11. L. FORNI, US Pat. 3 756 963, September 1973.
12. *Idem.*, US Pat. 3 758 416, September 1973.
13. L. FORNI, R. INVERNIZZI and C. GIANNINI, Ital. Pat. 984 025, November 1974.
14. L. FORNI and R. INVERNIZZI, US Pat. 3 853 786, December 1974.
15. L. FORNI, R. INVERNIZZI and L. V. MAO, *Chim. Ind. (Milan)* **57** (1975) 577.
16. L. FORNI and R. INVERNIZZI, US Pat. 4 029 719, June 1977.
17. L. FORNI, M. PELOZZI, A. GIUSTI, G. FORNASARI and R. MILLINI, *J. Catal.* **122** (1990) 44.
18. Eniricerche, Ital. Pat. 23 291A/85, December 1985.
19. Mobil, Brit. Pat. 1 402 981, January 1984.
20. G. PEREGO, G. BELLUSSI, C. CORNO, M. TARAMASSO, F. BUONOMO and A. ESPOSITO, in "New Developments in Zeolite Science and Technology", edited by Y. Murakami, A. Iijima and J. W. Ward (Elsevier, Amsterdam, 1986) p. 129.
21. G. PEREGO, personal communication (Sept. 1989).
22. M. TARAMASSO, G. PEREGO and B. NOTARI, in "Proceedings of the Fifth International Conference on Zeolites", edited by L. V. C. Rees (Heyden, London, 1980) p. 40.
23. H. M. RIETVELD, *J. Appl. Crystallogr.* **2** (1969) 65.
24. A. IMMIRZI, *Acta Crystallogr.* **B36** (1980) 2378.
25. D. H. OLSON, G. T. KOKOTAILO, S. L. LAWTON and W. M. MEIER, *J. Phys. Chem.* **85** (1981) 2238.
26. G. COUDURIER, C. NACCACHE and J. V. VEDRINE, *J. Chem. Soc. Chem. Commun.* (1982) 1413.
27. M. F. BEST and R. A. CONDRADE Jr, *J. Mater. Sci. Lett.* **4** (1985) 994.

Received 6 November  
and accepted 1 December 1989